Schrödinger-Poison Solvers Description and Quantum Corrections in classical simulators:

1. **Schrödinger-Poisson solvers**
   - major concerns for future integrated circuits
   - time-dependent Schrödinger wave equation (SWE)
   - discretization of the SWE for variable effective mass
   - time-independent Schrödinger equation
     - (A) Airy functions method
     - (B) Variational approach
     - (C) Shooting method for 1D problems – SCHRED description
     - (D) Finding the roots of a characteristic polynomial
     - (E) The Lanczos algorithm
     - (F) Numerov algorithm – note on the integration of the SWE
     - (G) 2D and 3D eigenvalue solvers
   - open systems
2. **The effective potential approach**
   - Madelung and Bohm's reformulation of quantum mechanics
   - other quantum potential formulations
   - the effective potential approach due to Ferry
   - simulation examples that utilize the effective potential approach
     - (A) Simulation of a 50 nm MOSFET device
     - (B) Simulation of a 250 nm FIBMOS device
     - (C) Simulation of a SOI device structure
   - conclusions regarding the use of the effective potential approach

1. Schrodinger-Poisson Solvers

1.1 Major concerns for future integrated circuits

- While current production devices are only at 0.1 μm, predictions are that they will be at 50 nm by year 2007. Issues that are currently investigated in these device structures include:
  - Tunnel currents in gate oxide
  - Source to drain tunneling
  - The role of the electron-electron interactions on carrier thermalization
  - Statistical fluctuations: gate-length, gate-width, oxide thickness and doping density variation:
    - Must go 3D instead of 2D
    - Must model ensemble of devices instead of a single device
    - Dopant solubility, activation and segregation at the surface must be addressed
- At these sizes, we should begin to see quantum effects, as λ_D~3-5 nm at 300 K. The questions are:
  - How large is the electron wave packet?
  - How do we include space quantization effect into classical device simulators?

Example 1: Degradation of C_{tot} for Different Device Technologies

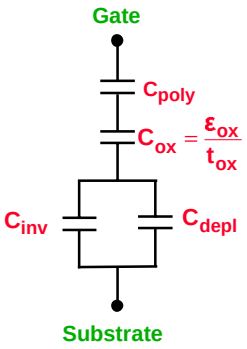

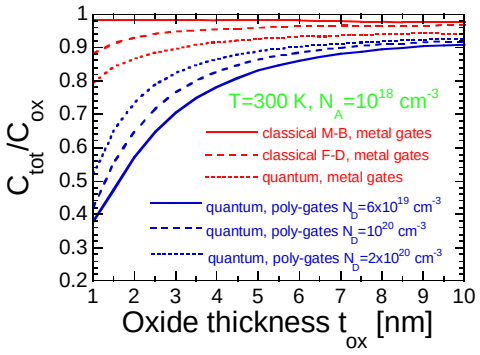

$$C_{tot} = \frac{C_{ox}}{1 + \frac{C_{ox}}{C_{poly}} + \frac{C_{ox}}{C_{inv} + C_{depl}}} \approx \frac{C_{ox}}{1 + \frac{C_{ox}}{C_{poly}} + \frac{C_{ox}}{C_{inv}}}$$

Conclusion: Quantization effects must be taken into account to properly describe the operation of future MOS devices.

Example 2: Heterojunction devices

- Esaki and Tsu (1969) => ionized donors can be spatially separated from the free electrons using modulation doping
- Dingle (1978) => grew the first modulation doped GaAs/AlGaAs superlattice

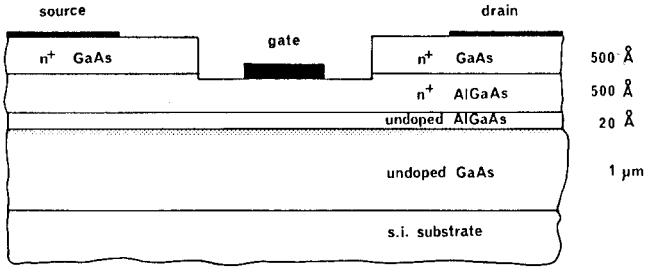

- The impact of the heterostructure is that the potential is abrupt, which leads to a more vigorous control of the channel charge density by the externally applied voltage.

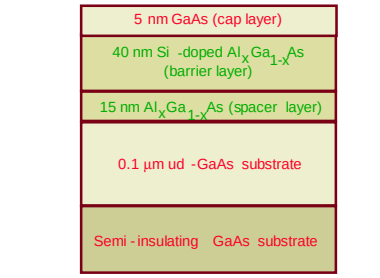

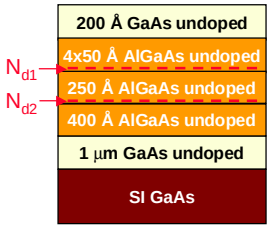

$N_{d1}=1x10^{12}$ cm^{-2} Si

$N_{d2}=3x10^{12}$ cm^{-2} Si

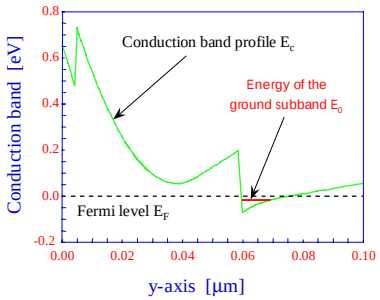

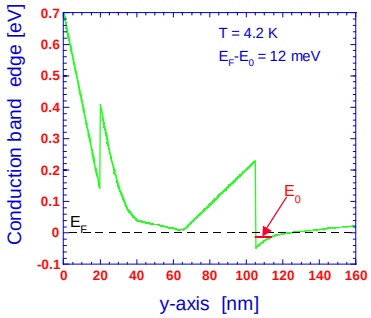

1.2 Time-dependent Schrödinger equation

- One of the goals of the quantum mechanics is to give quantitative description on a macroscopic scale of individual particles which behave both like particles and waves. The simplest wavefunction is a plane-wave:

$$\psi = \psi_0 \exp[i(\mathbf{k}\cdot\mathbf{r} - \omega t)], \quad \mathbf{p} = \hbar\mathbf{k} \quad \text{and} \quad E = \hbar\omega$$

- To describe realistic situations, more complicated wavefunctions can be constructed as superpositions of plane waves:

$$\psi(\mathbf{r},t) = \iiint d\mathbf{k}\psi_0(\mathbf{k})\exp\{i[\mathbf{k}\cdot\mathbf{r} - \omega(\mathbf{k})t]\}$$

- The evolution of the wavefunction is described by the time-dependent Schrödinger equation:

$$i\hbar\frac{\partial\psi(\mathbf{r},t)}{\partial t} = -\frac{\hbar^2}{2m}\nabla^2\psi(\mathbf{r},t) + V(\mathbf{r})\psi(\mathbf{r},t) \Rightarrow \psi(\mathbf{r},t) = \exp\left(-\frac{i}{\hbar}\mathbf{H}t\right)\psi(\mathbf{r},0)$$

- A stable and norm-preserving discretization scheme for the time-dependent SWE is the Crank-Nicholson semi-implicit scheme:

$$\frac{\psi^{K+1}-\psi^{K}}{\Delta t}=-\frac{i}{2\hbar}\left[H\psi^{K+1}+H\psi^{K}\right]\Rightarrow\psi^{K+1}=\frac{1-\frac{i}{2\hbar}H\Delta t}{1+\frac{i}{2\hbar}H\Delta t}\psi^{K}$$

- In the actual implementation, one solves the tri-diagonal system of equations

$$\left[\frac{2}{1+\frac{i}{2\hbar}H\Delta t}-1\right]\psi^{K}=\chi-\psi^{K}\Rightarrow\begin{aligned}2\psi_j^k&=-\frac{i\hbar\Delta t}{4mh^2}\chi_{j+1}-\frac{i\hbar\Delta t}{4mh^2}\chi_{j-1}\\&+\left(1+\frac{i\hbar\Delta t}{2mh^2}+\frac{i\Delta t}{2\hbar}V_j\right)\chi_{j+1}\end{aligned}$$

and then calculates the value of the wavefunction at time-step (*k+1*) as:

$$\psi^{k+1}=\chi^{k}-\psi^{k}$$

1.3 Discretization of the SWE for variable effective mass

- Under the assumption of slowly varying material composition, one can adopt the SWE with varying effective mass. There are two ways one can make the Hamiltonian of the system to be Hermitian:

(a) Bring the effective mass inside the differential operator, i.e.

$$H\psi=-\frac{\hbar^2}{2}\nabla\cdot\left(\frac{1}{m^*}\nabla\psi\right)+V\psi$$

For uniform mesh size, the discretized version of Hψ is:

$$-\frac{\hbar^2}{2\Delta^2}\left(\frac{\psi_{i+1}-\psi_i}{m^*_{i+1/2}}-\frac{\psi_i-\psi_{i-1}}{m^*_{i-1/2}}\right)+V_i\psi_i$$

(b) Another Hermitian operator proposed for variable mass has the form:

$$H\psi = -\frac{\hbar^2}{4}\left[\frac{1}{m^*}\nabla^2\psi + \nabla^2\left(\frac{1}{m^*}\psi\right)\right] + V\psi$$
$$= -\frac{\hbar^2}{2}\left[\frac{1}{m^*}\frac{\partial^2\psi}{\partial z^2} + \frac{\partial\psi}{\partial z}\frac{\partial}{\partial z}\left(\frac{1}{m^*}\right) + \frac{1}{2}\psi\frac{\partial^2}{\partial z^2}\left(\frac{1}{m^*}\right)\right] + V\psi$$

If one applies the box-integration method to the first two terms of this Hamiltonian, it gives the same discretized form of the equations as the fist method

$$\int_{i-1/2}^{i+1/2}\frac{1}{m^*}\frac{\partial^2\psi}{\partial z^2}dz + \int_{i-1/2}^{i+1/2}\frac{\partial\psi}{\partial z}\frac{\partial}{\partial z}\left(\frac{1}{m^*}\right) = \frac{1}{m^*}\frac{\partial\psi}{\partial z}\Big|_{i-1/2}^{i+1/2}$$
$$-\int_{i-1/2}^{i+1/2}\frac{\partial\psi}{\partial z}\frac{\partial}{\partial z}\left(\frac{1}{m^*}\right) + \int_{i-1/2}^{i+1/2}\frac{\partial\psi}{\partial z}\frac{\partial}{\partial z}\left(\frac{1}{m^*}\right) = \frac{1}{m^*}\frac{\partial\psi}{\partial z}\Big|_{i-1/2}^{i+1/2}$$

1.4 Time-independent Schrödinger equation

- If one is considering stationary states, then:

$$\psi(\mathbf{r},t) = \psi(\mathbf{r})\exp(-i\omega t) = \psi(\mathbf{r})\exp(-iEt/\hbar)$$

- The time-independent SWE then reduces to:

$$-\frac{\hbar^2}{2m^*}\nabla^2\psi(\mathbf{r}) + V(\mathbf{r})\psi(\mathbf{r}) = E\psi(\mathbf{r})$$

  (a) For a system confined by a potential well, the SWE is an eigenvalue problem

  (b) For an open system, one has a boundary value problem where the energy of the wanted solution is specified and one has to specify the spatial variation of $\psi(\mathbf{r})$

- For 1D confinement (triangular or rectangular quantum well problems) one can use either:
  - analytical approaches
  - numerical approaches

- Summary of approaches used to solve the SWE

Triangular well (analytical approaches) → Airy functions method
Triangular well (analytical approaches) → Variational Approach

Numerical Approaches → **1D**
1. Shooting method
2. Finding the roots of a characteristic polynomial
3. Lanczos algorithm

Numerical Approaches → **2D and 3D**
1. Housholder method
2. Implicitly restarted Arnoldi method (ARPACK)

(A) Airy functions method

- Suppose, we want to solve self-consistently the 1D Schrödinger-Poisson problem in a MOS structure:

$$-\frac{\hbar^2}{2m^*}\frac{\partial^2\psi(z)}{\partial z^2}+V(z)\psi(z)=E\psi(z)$$

$$\frac{\partial^2 V}{\partial z^2}=-\frac{e}{\varepsilon}(N_A+n),\quad n=\sum_i N_i\psi_i^2(z)$$

- The analytical solution of the Poisson equation is of the form:

$$V(z)=\frac{e^2N_AW}{\varepsilon}z\left(1-\frac{z}{2W}\right)+\frac{e^2}{\varepsilon}\sum_i N_i\left[z-\int_0^z(z-z')\psi_i^2(z')dz'\right]$$

$$W=\sqrt{\frac{2\varepsilon E_d}{e^2N_A}},\quad E_d=(E_c-E_F)_{bulk}+(E_F-E_0)+E_0-\frac{e^2N_s\langle z\rangle_{av}}{\varepsilon}$$

- When the inversion charge density does not make significant contribution to the band-bending, The 1D SWE reduces to:

$$-\frac{\hbar^2}{2m^*}\frac{\partial^2\psi(z)}{\partial z^2}+eF_s z\psi(z)=E\psi(z),\quad F_s=\frac{eN_AW}{\varepsilon}$$

- The solutions are:

$$\psi_i(z)=Ai\left[\frac{2m^*eE_s}{\hbar^2}\left(z-\frac{E_i}{eF_s}\right)\right]$$

$$E_i\approx\left(\frac{\hbar^2}{2m^*}\right)^{1/3}\left[\frac{3\pi eF_s}{2}\left(i+\frac{3}{4}\right)\right]^{2/3}$$

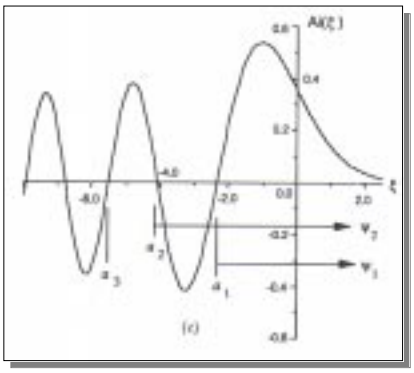

(B) Variational Approach

- When the electrons significantly affect the band bending near the interface, the Airy functions approach fails. In this case, at low temperatures one can use the variational approach due to Fang and Howard, in which the ground state wavefunction is assumed to be of the form:

$$\psi_0(z)=\sqrt{\frac{b^3}{2}}ze^{-bz/2}$$

- The energy of the lowest subband is:

$$<E_o>=<T>+<V_d>+<V_s>+<V_I>$$

$$\frac{\hbar^2b^2}{8m^*}\qquad \frac{3e^2N_AW}{\varepsilon_{sc}b}-\frac{6e^2N_A}{\varepsilon_{sc}b^2}\qquad \frac{33e^2N_s}{16\varepsilon_{sc}b}\qquad \frac{\varepsilon_{sc}-\varepsilon_{ox}}{\varepsilon_{sc}+\varepsilon_{ox}}\frac{e^2b}{32\pi\varepsilon_{sc}}$$

- When one minimizes the total energy per electron, it follows that:

$$b = \left[\frac{12m^* e^2 N^*}{\varepsilon_{sc}\hbar^2}\right], \quad \text{where} \quad N^* = N_{depl} + \frac{11}{32}N_s$$

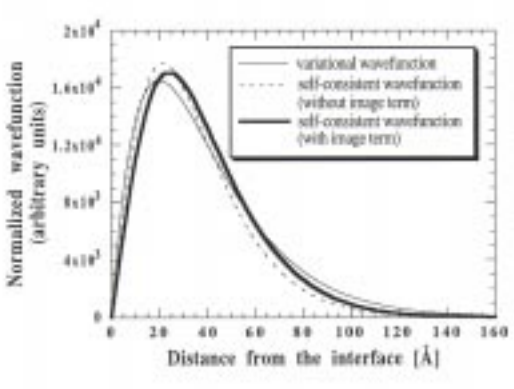

$N_A = 10^{15}\ cm^{-3}$
$N_s = 10^{12}\ cm^{-2}$
$T = 0K$

(C) Shooting Method for 1D problems

- To describe the shooting method, lets rewrite the time-independent SWE in the form:

$$\frac{d^2\psi}{dz^2} + k^2(z)\psi(z) = 0, \quad k(z) = \sqrt{\frac{2m^*}{\hbar^2}[E - V(z)]}$$

- When discretized on a uniform mesh, one gets that:

$$\psi_{i+1} - \left(2 - k_i^2\Delta^2\right)\psi_i + \psi_{i-1} = 0$$

- The schematics of the potential used in the discussion is:

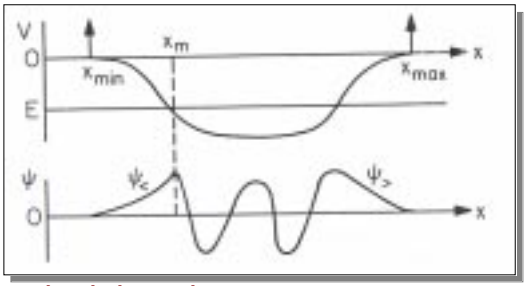

- The solution strategy is the following one:

(1) Integrate the SWE towards larger z from z_{min}

$$\psi_{i+1} = (2 - k_i^2 \Delta^2)\psi_i - \psi_{i-1}$$

(2) Integrate the SWE towards smaller z starting from z_{max}

$$\psi_{i-1} = (2 - k_i^2 \Delta^2)\psi_i - \psi_{i+1}$$

(3) At the matching point z_m, one matches the solutions $\psi^<$ and $\psi^>$

(4) The eigenvalue is then signaled by equality of the derivatives at z_m

$$\left.\frac{d\psi^<}{dz}\right|_{z_m} = \left.\frac{d\psi^>}{dz}\right|_{z_m} \quad \Rightarrow \quad f = \frac{1}{\psi}\left[\psi^<(z_m - \Delta) - \psi^>(z_m - \Delta)\right]$$

(C1) Description of SCHRED

- For actual device simulations, one has to solve self-consistently the 1D Schrödinger equation self-consistently with the 1D Poisson equation.
- For the case of Si, in the solution of the 1D Schrödinger equation one must worry about the mass anisotropy

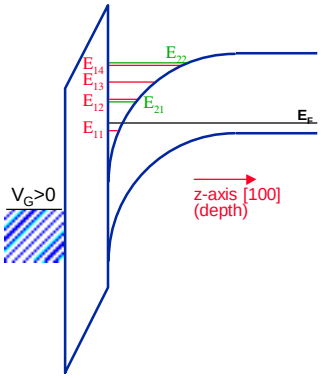

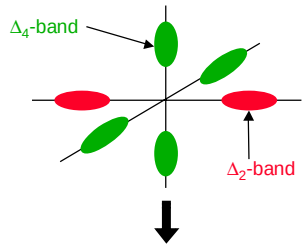

Δ_2-band:
$m_\perp = m_l = 0.916 m_0$, $m_{||} = m_t = 0.196 m_0$

Δ_4-band:
$m_\perp = m_t = 0.196 m_0$, $m_{||} = (m_l\, m_t)^{1/2}$

(1) Existing Features of SCHRED:

1. Classical and quantum-mechanical charge description
   - → Fermi-Dirac and Maxwell-Boltzmann statistics
2. Single-valley and multiple-valley conduction bands
3. Exchange and correlation corrections to the ground state energy of the system
4. Metal and poly-silicon gates
5. Partial ionization of the impurity atoms

Features Recently Being Implemented in SHRED:

- Hole quantization
- Non-parabolicity of the bands

Current home of the solver: Purdue Semiconductor Simulation Hub (http://www.ecn.purdue.edu/labs/punch/)

(2) Sample input file used in SCHRED simulations:

```
device      bulk=yes
params      temp[K]=300, tox[nm]=1.5, kox=3.9
body        uniform=true, Nb[cm-3]=1.e19
gate        metal=false, Ng[cm-3]=-6.0e19
ionize      ionize=no, Ea[meV]=45, Ed[meV]=45
voltage     Vmin[V]=0, Vmax[V]=2.5, Vstep[V]=0.1
charge      quantum=yes, Fermi=yes, exchange=no,
+           e_nsub1=4, e_nsub2=2
calc        CV_curve=yes, file_cv=cv.dat
save        charges=no, file_ch=chrg.dat,
+           wavefunc=no, file_wf=wfun.dat
converge    toleranc=5.e-6, max_iter=2000
```

(3) Sample of simulation results obtained with SCHRED:

$$E = E^{HF} + E_{corr} = E^{HF}_{kin} + E^{HF}_{exchange} + E_{corr}$$

- E: Total Ground State Energy of the System
- E^{HF}: Hartree-Fock Approximation for the Ground State Energy
- E_{corr}: Accounts for the error made with the Hartree-Fock Approximation
- $E^{HF}_{exchange} + E_{corr}$: Accounts for the reduction of the Ground State Enery due to the inclusion of the Pauli Exclusion Principle

Vasileska *et al.*, J. Vac. Sci. Technol. B **13**, 1841 (1995)
(N_a=2.8x10^{15} cm^{-3}, N_s=4x10^{12} cm^{-2}, T=0 K)

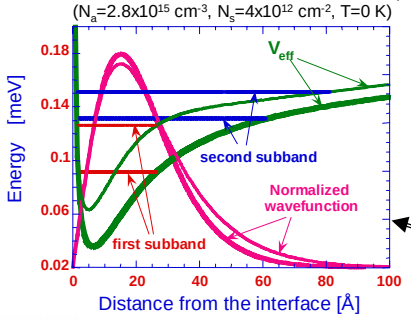

Exchange-Correlation Correction:

- ⇨ Lower subband energies
- ⇨ Increase in the subband separation
- ⇨ Increase in the carrier concentration at which the Fermi level crosses into the second subband
- ⇨ Contracted wavefunctions

Thick (thin) lines correspond to the case when the exchange-correlation corrections are included (omitted) in the simulations.

(4) Sample of simulation results obtained with SCHRED (Cont'd):

Kneschaurek *et al.*, Phys. Rev. B **14**, 1610 (1976)

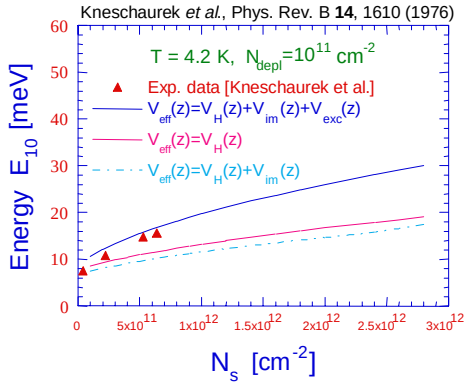

Infrared Optical Absorption Experiment:

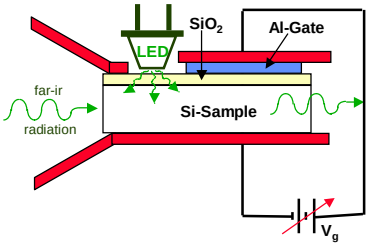

Transmission-Line Arrangement

(4) Sample of simulation results obtained with SCHRED (Cont'd):

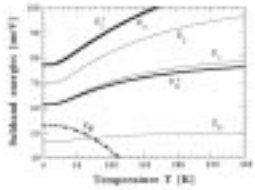

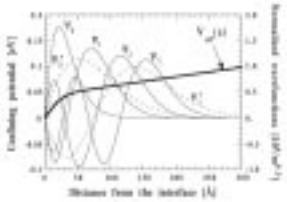

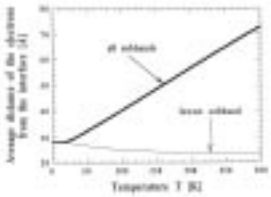

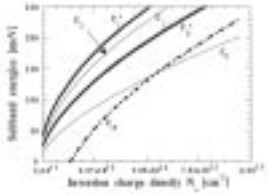

(D) Finding the roots of a characteristic polynomial

- The finite-difference approximation of the 1D SWE is given by:

$$\frac{d^2\psi}{dz^2} + V(z)\psi(z) = E\psi(z)$$

$$\frac{1}{\Delta^2}\psi_{i-1} + \left(V_i - \frac{2}{\Delta^2}\right)\psi_i + \frac{1}{\Delta^2}\psi_{i+1} = E\psi_i$$

$$\Downarrow$$

$$A_{i,i-1}\psi_{i-1} + A_{i,i}\psi_i + A_{i,i+1}\psi_{i+1} = E\psi_i$$

- The eigenvalues are the zeroes of the N[th] degree characteristic polynomial of **A**

$$P_A(E) = \det(\mathbf{A} - E\mathbf{I}) = \prod_{i=1}^{N}(E_i - E)$$

$$\Downarrow$$

$$P_1(E) = A_{1,1} - E\,, \quad P_2(E) = (A_{2,2} - E)P_1(E) - A_{1,2}^2\,,$$

$$P_n(E) = (A_{n,n} - E)P_{n-1}(E) - A_{n,n-1}^2 P_{n-2}(E)$$

- Several features help considerably in finding the roots of P_A:

  (1) The number of times the sequence 1, $P_1(E)$, $P_2(E)$,…,$P_N(E)$ changes sign equals the number of eigenvalues less than E

  (2) To make a systematic search for all of the eigenvalues, a guidance can be the Gerschgorin's bounds:

$$E_n \geq \min_i \left\{ A_{i,i} - \sum_{j \neq i} |A_{i,j}| \right\}; \quad E_n \leq \max_i \left\{ A_{i,i} + \sum_{j \neq i} |A_{i,j}| \right\};$$

  (3) Once the eigenvalues are determined, the eigenvectors are found by using the inverse vector iteration procedure, in which one starts with an initial guess for the eigenvector $\psi_n^{(1)}$ associated with a given eigenvalue E_n and refines the guess by evaluating:

$$\psi_n^{(2)} = [\mathbf{A} - (E_n + \delta)\mathbf{I}]^{-1} \psi_n^{(1)}$$

(E) The Lanczos algorithm

- This algorithm is very suitable when one is interested in many of the lowest eigenvalues.
- The strategy is to construct a set of orthonormal basis vectors $\{\psi_n\}$, in which **A** is explicitly tri-diagonal matrix

  (1) Choose an arbitrary first vector in the basis ψ_1 such that:

$$\psi_1^T \psi_1 = 1$$

  (2) One then forms a second vector in the basis as:

$$\psi_2 = C_2(\mathbf{A}\psi_1 - A_{11}\psi_1)$$

$$A_{11} = \psi_1^T \mathbf{A} \psi_1, \quad C_2 = \left[(\mathbf{A}\psi_1)^T (\mathbf{A}\psi_1) - A_{11}^2 \right]^{-1/2}$$

  (3) Subsequent vectors in the basis are then constructed recursively:

$$\psi_{n+1} = C_{n+1}(\mathbf{A}\psi_n - A_{nn}\psi_n - A_{nn-1}\psi_{n-1})$$

$$C_{n+1} = \left[(\mathbf{A}\psi_n)^T (\mathbf{A}\psi_n) - A_{nn}^2 A_{nn-1}^2 \right]^{-1/2}$$

- The real utility of the Lanczos method is when many, but bot all, of the eigenvalues of a large matrix are required. Suppose that one is interested in the 10 lowest eigenvalues of a matrix of dimension 1000. The procedure is then the following:

  (1) Generate some number of states in a basis larger than the number of eigenvalues being sought

  (2) A linear combination of these eigenvectors is then used in constructing a new basis of dimension 25

  (3) The continued procedure of:

  -> generating a limited basis,

  -> diagonalizing the tridiagonal matrix

  -> using the normalized sum of the lowest eigenvectors as the first vector in the next basis

  converges to the required eigenvalues and eigenvectors.

(F) Numerov Algorithm – note on the integration of the SWE

- There is particularly simple and efficient method for integrating second-order differential equations called Numerov or Cowling's method, based on the idea sketched below:

$$\frac{\psi_{i-1}-2\psi_i+\psi_{i+1}}{\Delta^2}=\psi_i''+\frac{\Delta^2}{12}\psi_i''''$$

$$\frac{\partial^2}{\partial x^2}\left(\frac{\partial^2\psi}{\partial x^2}\right)=\frac{\partial^2}{\partial x^2}\left(-k^2\psi\right)=-\frac{\left(k^2\psi\right)_{i-1}-2\left(k^2\psi\right)_i+\left(k^2\psi\right)_{i+1}}{\Delta^2}$$

$$\left(1+\frac{\Delta^2}{12}k_{i+1}^2\right)\psi_{i+1}-2\left(1-\frac{5\Delta^2}{12}k_i^2\right)\psi_i+\left(1+\frac{\Delta^2}{12}k_{i-1}^2\right)\psi_{i-1}=0$$

- Solving the linear system of equations for either ψ_{i-1} or ψ_{i+1} then provides a recursion relation for integrating either forward or backward

(G) 2D and 3D Eigenvalue Solvers

- When solving 2D eigenvalue problems, one can transform the matrix to tri-diagonal form by using either the Householder method, Lanczos iteration or Rayleigh quotient iteration method (S.E. Laux, and F. Stern, Appl. Phys. Lett. 49, pp. 91, 1986).
- For 3D problems, the **best** eigenvalue solvers of large and sparce matrices, based on Implicitly Restarted Arnoldi Method, can be found in the publicly available software package ARPACK:

  -> the codes are available by anonymous ftp from

  ftp.caam.rice.edu

  -> or by connecting directly to the URL

  http://www.caam.rice.edu/software/ARPACK

1.5 Open Systems

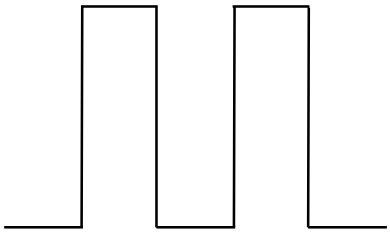

To calculate the conduction-band edge of the RTD structure, one needs to solve self-consistently the Poisson equation:

$$\nabla^2\varphi = -\frac{e}{\varepsilon}\left(N_D - N_A - n\right)$$

and the 1D Schrödinger equation:

$$-\frac{\hbar^2}{2m}\frac{\partial^2\psi}{\partial x^2} + E_c(x)\psi(x) = E\psi(x)$$

$$\Downarrow$$

$$\frac{\partial^2\psi}{\partial x^2} + \frac{2m}{\hbar^2}\left[E - E_c(x)\right]\psi(x) = 0 \Rightarrow \frac{\partial^2\psi}{\partial x^2} + k_x^2(x)\psi(x) = 0$$

- For a 1D domain limited to $x \in [0, L]$, the SWE discretized on a uniform grid, with mesh size Δ is:

$$\frac{\psi_{i-1} - 2\psi_i + \psi_{i+1}}{\Delta^2} + k_i^2 \psi_i = 0$$

- The traveling wave at a specified energy is assumed to be of a plane-wave type of the form:

$$\psi(x) = A(x)\exp[\pm jxk(x)]$$

- For a traveling wave that enters the open system at x=0, the procedure is the following one:

  (1) one sets A(L)=1 at the output boundary to get that:

$$\psi_N = \exp(jk_N L)$$
$$\psi_{N+1} = \exp[jk_N(L+\Delta)] = \psi_N \exp(jk_N \Delta)$$

(2) The next step is to calculate the wavefunction for i=0,1,…, N-1:

$$\psi_{i-1} = \left[2 - \Delta^2 k_i^2\right]\psi_i - \psi_{i+1}$$

(3) For i=0, one has that:

$$\psi_0 = I_0 + R_0;\ \psi_{-1} = I_0 \exp(-jk_0\Delta) + R_0 \exp(jk_0\Delta)$$

$$I_0 = \frac{\psi_0 \exp(jk_0\Delta) - \psi_{-1}}{i2\sin(jk_0\Delta)}$$

- The procedure for inflow from the right boundary is identical:

$$\psi_{i+1} = \left[2 + \frac{2m\Delta^2}{\hbar^2}(V_i - E)\right]\psi_i - \psi_{i-1}$$

and is started assuming $\psi_0 = 1$ and $\psi_{-1} = \exp(-jk_0\Delta)$.

- To find the total wavefunction from the renormalized results of the two recursions steps (from the left and from the right), one needs to specify the INJECTION conditions:

$$n(x)=\int_{-\infty}^{+\infty}\frac{dk_x}{2\pi}n(k_x) \quad \textbf{where} \quad n(k_x)=\frac{m}{\pi\hbar^2}\ln\left[1+\exp\left(\frac{E_F-E_{CL}-E_x}{k_BT}\right)\right]$$

- Once the wavefunction is determined, one can proceed with the calculation of the current through the structure:

$$J(x)=-\frac{e\hbar}{2\pi m}\sum_{k_j}n(k_j)\left[\psi^*(k_j)\frac{\partial\psi(k_j)}{\partial x}-\psi(k_j)\frac{\partial\psi^*(k_j)}{\partial x}\right]\Delta k$$

- The electron density is then given by:

$$n(x)=\frac{1}{2\pi}\sum_{k_j}n(k_j)\psi^*(k_j)\psi(k_j)\Delta k$$

2. The effective potential approach

2.1 Madelung and Bohm's Reformulation of QM

- The hydrodynamic formulation is initiated by substituting the wavefunction into the time-dependent SWE:

$$\psi=Re^{iS/\hbar} \quad , \quad R=\sqrt{n}=|\psi| \quad \rightarrow \quad -\frac{\hbar^2}{2m}\nabla^2\psi+V\psi=i\hbar\frac{\partial\psi}{\partial t}$$

- The resultant real and imaginary parts give:

$$(1)\quad \frac{\partial\rho(\mathbf{r},t)}{\partial t}+\nabla\cdot\left(\rho\frac{1}{m}\nabla S\right)=0; \quad \rho(\mathbf{r},t)=R(\mathbf{r},t)^2; \quad \mathbf{v}=\nabla S/m$$

$$(2)\quad -\frac{\partial S(\mathbf{r},t)}{\partial t}=\frac{1}{2m}(\nabla S)^2+V(\mathbf{r},t)+Q(\rho,\mathbf{r},t); \quad \textbf{Hamilton Jacobi eq.}$$

$$\downarrow$$

$$Q(\rho,\mathbf{r},t)=-\frac{\hbar^2}{2m}\frac{1}{R}\nabla^2R=-\frac{\hbar^2}{2m}\rho^{-1/2}\nabla^2\rho^{1/2}$$

$$m\frac{d\mathbf{v}}{dt}=-\nabla(V+Q)=f_c+f_q$$

2.2 Other Quantum Potential Formulations

- An alternate form of the quantum potential has been proposed by ***Iafrate, Grubin and Ferry***, and is based on moments of the Wigner-Boltzmann equation:

$$V_Q = -\frac{\hbar^2}{8m}\frac{\partial^2(\ln n)}{\partial x^2}$$ ← Wigner potential or density-gradient correction

- ***Ferry and Zhou*** derived a form for a smooth quantum potential based on the effective classical partition function of Feynman and Kleinert. The ***Feynman and Kleinert*** idea is as follows:

  (a) Calculate the smeared version of the potential $V(x)$ as follows:

$$V_{a^2}(x) = \int \frac{dx'}{\left(2\pi a^2\right)^{1/2}} \exp\left[-\frac{1}{2a^2}(x-x')^2\right] V(x')$$

  (b) Introduce a second parameter Ω and form the auxiliary potential:

$$\tilde{W}(x, a^2, \Omega) = \frac{1}{\beta}\ln\frac{\sinh(\beta\Omega/2)}{\beta\Omega/2} - \frac{\Omega^2}{2}a^2 + V_{a^2}(x')$$

(c) The minimization with respect to Ω and the minimization with respect to a^2 then give:

$$a^2 = \frac{1}{\beta\Omega^2}\left[\frac{\beta\Omega}{2}\coth\left(\frac{\beta\Omega}{2}\right) - 1\right] \quad \text{and} \quad \Omega^2(x_0) = 2\frac{\partial}{\partial a^2}V_{a^2}(x_0)$$

- ***Gardner and Ringhofer*** derived a smooth quantum potential for hydrodynamic modeling that is valid to all orders of $\hbar^2$, that involves smoothing integration of the classical potential over space and temperature:

$$V(\beta, x) = \int_0^\beta \frac{d\beta'}{\beta}\left(\frac{\beta'}{\beta}\right)^2 \int d^3x' \left[\frac{2m\beta}{\pi(\beta-\beta')(\beta+\beta')\hbar^2}\right] \times \exp\left\{-\frac{2m\beta}{\pi(\beta-\beta')(\beta+\beta')\hbar^2}(\mathbf{x}'-\mathbf{x})^2\right\} V(\mathbf{x}')$$

2.3 The Effective Potential Approach due to *Ferry*

In principle, the effective role of the potential can be rewritten in terms of the non-local density as (Ferry *et al.*[1]):

$$\bar{V} = \int dr V(\mathrm{r}) \sum_i n_i(\mathrm{r})$$

$$\sim \int dr V(\mathrm{r}) \sum_i \int d\mathrm{r}' \exp\left(-\frac{|\mathrm{r}-\mathrm{r}'|^2}{\alpha^2}\right) \delta(\mathrm{r}'-\mathrm{r}_i)$$

$$\sim \sum_i \int dr \delta(\mathrm{r}-\mathrm{r}_i) \int d\mathrm{r}' V(\mathrm{r}') \exp\left(-\frac{|\mathrm{r}-\mathrm{r}'|^2}{\alpha^2}\right)$$

$$\sim \sum_i \int dr \delta(\mathrm{r}-\mathrm{r}_i) V_{eff}(\mathrm{r})$$

Classical density

Smoothed, effective potential

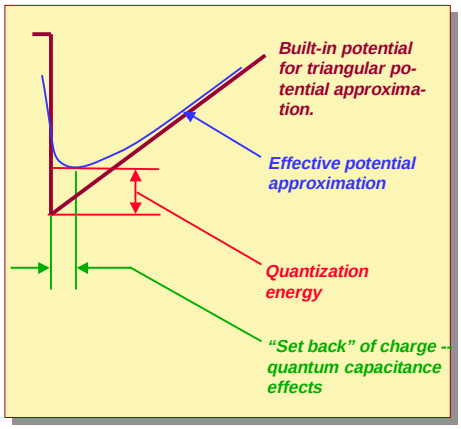

[1] D. K. Ferry, *Superlatt. Microstruc.* **27**, 59 (2000); *VLSI Design*, in press.

- The connection of Ferry's Approach to the Bohm Potential is given below:

$$V_{eff}(x) = \frac{1}{\sqrt{2\pi}\alpha} \int_{-\infty}^{\infty} V(x+\xi) e^{-\xi^2/2\alpha^2} d\xi$$

$$\cong \frac{1}{\sqrt{2\pi}\alpha} \int_{-\infty}^{\infty} \left[V(x) + \xi \frac{\partial V}{\partial x} + \frac{\xi^2}{2} \frac{\partial^2 V}{\partial x^2} + \ldots \right] e^{-\xi^2/2\alpha^2} d\xi.$$

$$V_{eff}(x) = V(x) + \alpha^2 \frac{\partial^2 V}{\partial x^2} + \ldots.$$

$$V_{eff}(x) = V(x) - \frac{2\alpha^2}{\beta} \frac{\partial^2 \ln(\sqrt{n/n_0})}{\partial x^2} + \ldots$$

$$= V(x) - \frac{2\alpha^2}{\beta\sqrt{n}} \frac{\partial^2 \sqrt{n}}{\partial x^2} + \ldots.$$

$$Q = \frac{\hbar^2}{2m^*} \frac{\nabla^2 |\psi|}{|\psi|}$$

In semiconductors, typically the dependence of the density upon the potential is as a factor *exp(-βV)*

Within a factor of 2, the second term is now recognized as the density gradient term, but is more commonly known as the ***Bohm potential***

(1) Validation of the approach on the example of a MOS capacitor with t_{ox} = 6 nm – sheet density results:

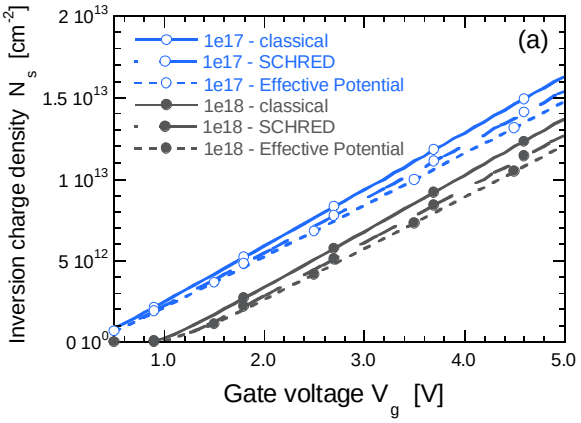

The Gaussian fitting parameter a_0 = 0.5 nm.

(2) Validation of the approach on the example of a MOS capacitor with t_{ox} = 6 nm – results for the average carrier displacement:

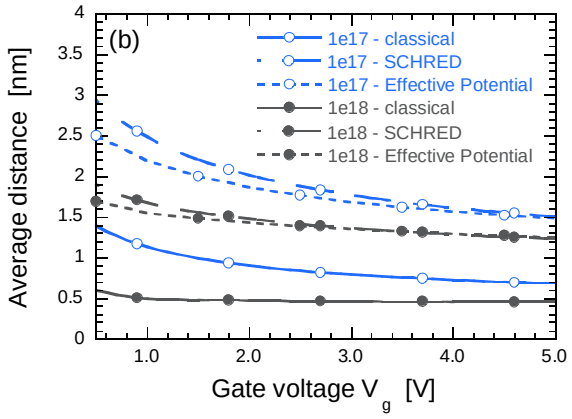

The Gaussian fitting parameter a_0 = 0.5 nm.

2.4 Simulation examples that utilize the effective potential approach

(A) Simulation of a 50 nm MOSFET Device

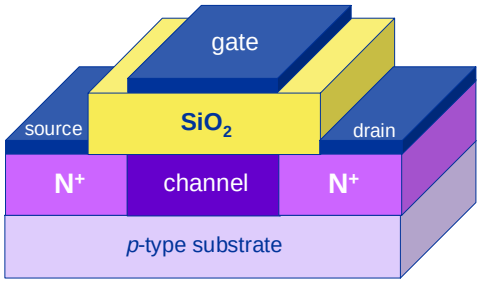

Device specification:

- Oxide thickness = 2 nm
- Channel length = 50 nm
- Channel width = 0.8 μm
- Junction depth = 36 nm
- Substrate doping:
  $N_A=10^{18}$ cm^{-3}
- Doping of the source-drain regions:
  $N_D = 10^{19}$ cm^{-3}

(1) Conduction Band Profile

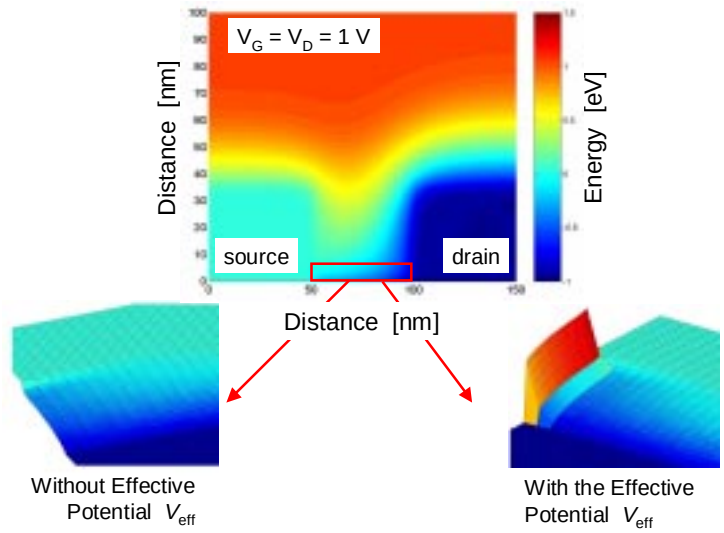

(2) Electric field profile

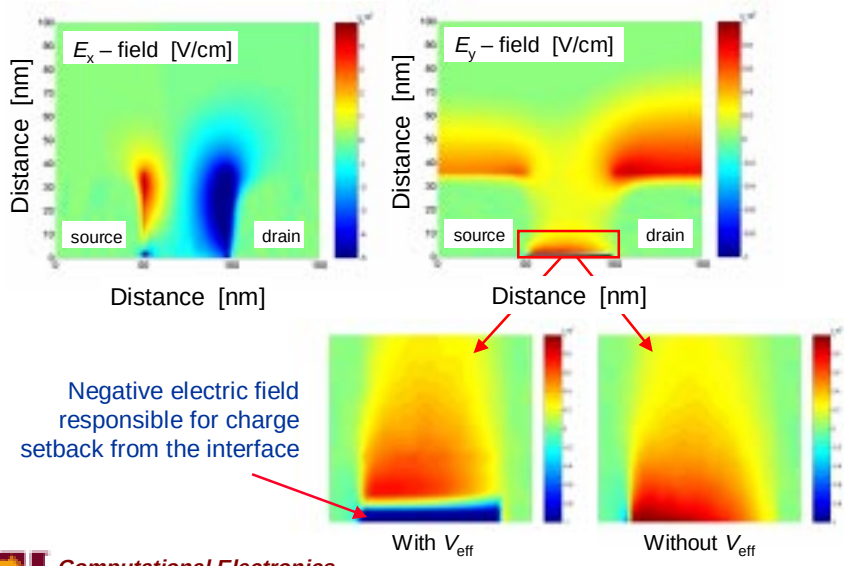

Computational Electronics

(3) Carrier density and average distance

Applied bias: V_G = 1 V

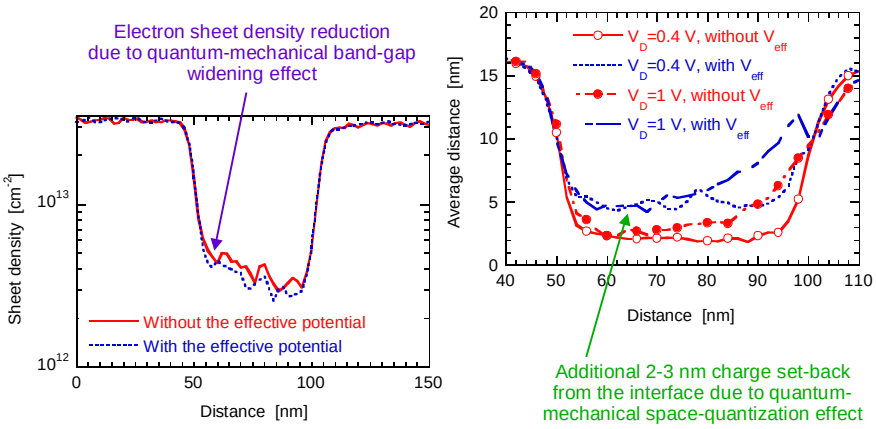

Computational Electronics

(4) Transfer and output characteristics

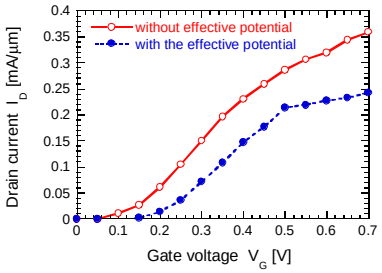

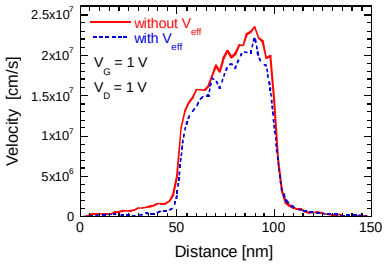

- The observed threshold voltage shift is mainly due to the degradation of the device transconductance and is not due to mobility degradation in the channel.
- The shift in the threshold voltage leads to a reduction in the on-state current.

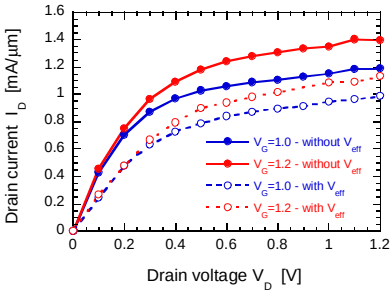

(B) Simulation of a 250 nm FIBMOS device

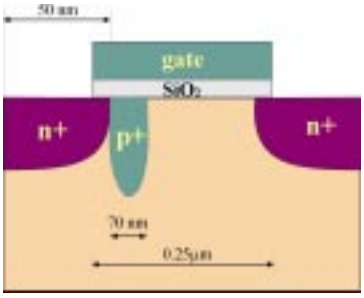

Source and drain length	50 nm
Source and drain junction depth	36 nm
Gate length	250 nm
Device width	1.4 μm
Bulk depth	400 nm
Oxide thickness	5 nm
Source and drain doping	10^{19} cm^{-3}
Substrate doping	10^{16} cm^{-3}
Implant doping	1.6×10^{18} cm^{-3}
Substrate doping	10^{16} cm^{-3}
Implant length	70 nm

(1) Concentration of electrons in the channel

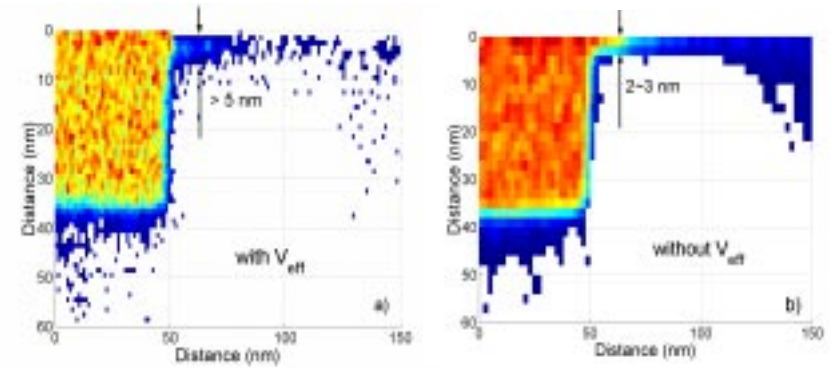

Average electron displacement from the interface and the total channel width increase when quantum effects are included!

(2) Sheet electron density

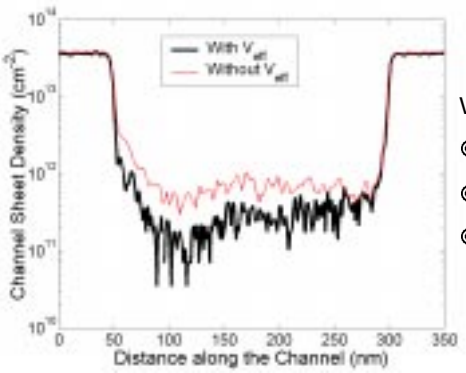

When Quantum effects are included:

- sheet density is reduced
- inversion more difficult to achieve
- threshold voltage is increased

(3) Energy and velocity along the channel

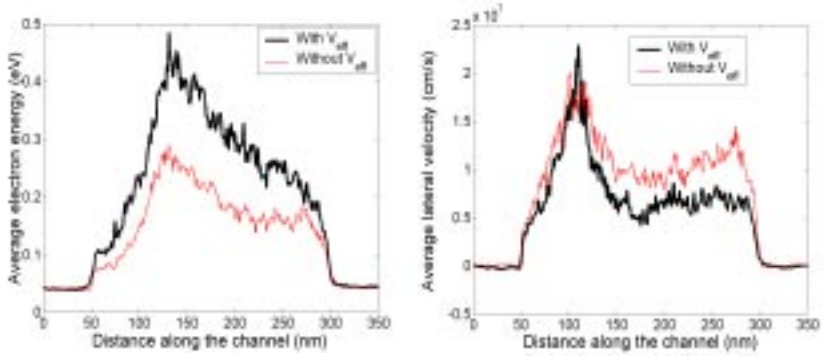

- Average energy increases and velocity decreases when quantum effects are included.
- Prominent velocity overshoot evidence of non-stationary transport.

(4) Device transfer and output characteristics

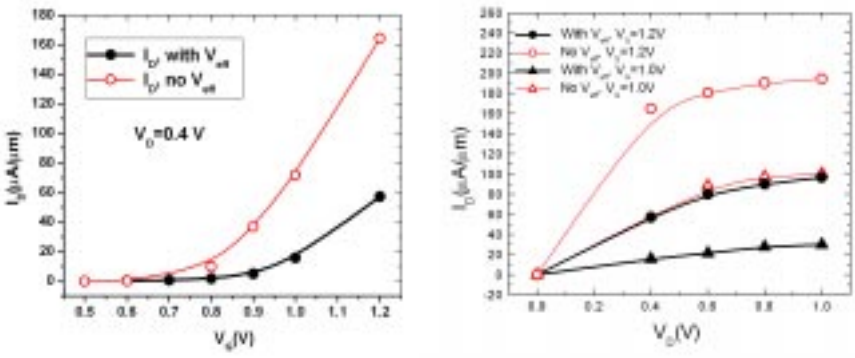

With quantum effects:

- Drive current is lowered
- Threshold voltage is higher
- Transconductance is degraded

(C) Simulation of a SOI Device Structure

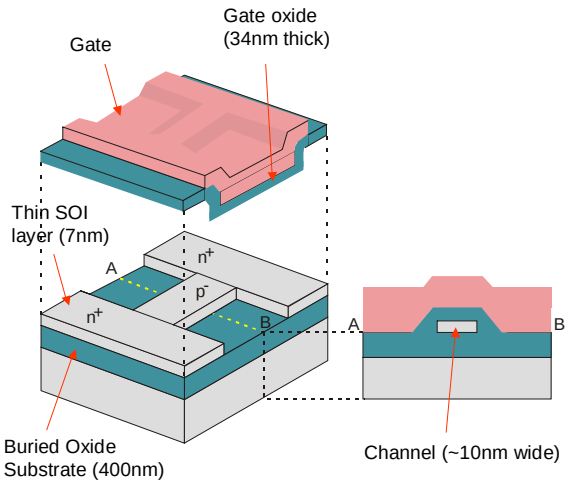

Experimental data[1]:

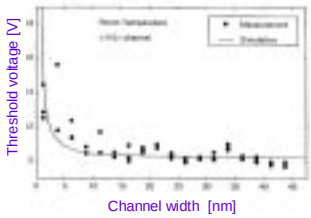

- Simulate this structure using full 3D Poisson solver coupled with 2D Schrödinger solver.
- Do the same calculation with effective potential

[1] Majima, Ishikuro, Hiramoto, *IEEE El. Dev. Lett.* **21**, 396 (2000).

(1) Proof of concept for 2D quantization

Approach 1:

Solve the 2D Schrödinger equation

$$\left[-\frac{\hbar^2}{2m_y^{\nu}}\frac{\partial^2}{\partial y^2}-\frac{\hbar^2}{2m_z^{\nu}}\frac{\partial^2}{\partial y^2}+V(x,y,z)\right]\psi_j^{\nu}(x,y,z)=E_j^{\nu}(x)\psi_j^{\nu}(x,y,z)$$

where the electron density is given by:

$$n(x,y,z)=2\sum_{\nu=1}^{3}\sum_j N_j^{\nu}(x)\left|\psi_j^{\nu}(x,y,z)\right|^2;\quad N_j^{\nu}(x)=\frac{1}{\pi\hbar}\sqrt{2m_x^{\nu}k_BT}\cdot F_{-1/2}\left(\frac{E_j^{\nu}(x)-E_F}{k_BT}\right)$$

Approach 2:

Use the effective potential approach to obtain the line electron density.

(2) Simulation results for a quantum wire

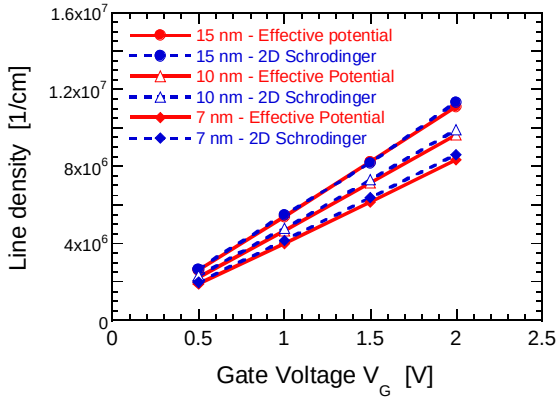

Excellent agreement is observed between the two approaches when using the theoretical value for the Gaussian smoothing parameter of 0.64 nm.

2.5 Conclusions regarding the use of the effective potential approach

- The effective potential approach in many cases allows for a quite accurate approximation of the quantization effects in real semiconductor devices
- The numerical cost of including the effective potential is low – "more bang for the buck"

Some challenges remain, however:

- Model valid within the random phase approximation.
- It is still "quasi-local", so it does not allow proper treatment phase interference effects